Numerical Methods in Radiation Room Shielding

Ashtan Mistal

Introduction

- The goal of the design of a radiation treatment room is to minimize the dose to areas that are not directly being treated. This is done by shielding the room from the radiation source using materials that absorb radiation.
- The shielding is designed to minimize the dose to staff working in the room and to minimize the dose to areas surrounding the room. The Monte Carlo (MC) method has been proven to be one of the most accurate methods in determine dose calculations for treatment planning, dosimetry, and in the design of treatment devices [12, 6].
- With primary radiation being absorbed by the patient, the radiation that is of interest to us is the secondary radiation (the radiation that is scattered by the patient) and the tertiary radiation (the scattered radiation by the walls, floor, ceiling, and surrounding air of the room) [5].

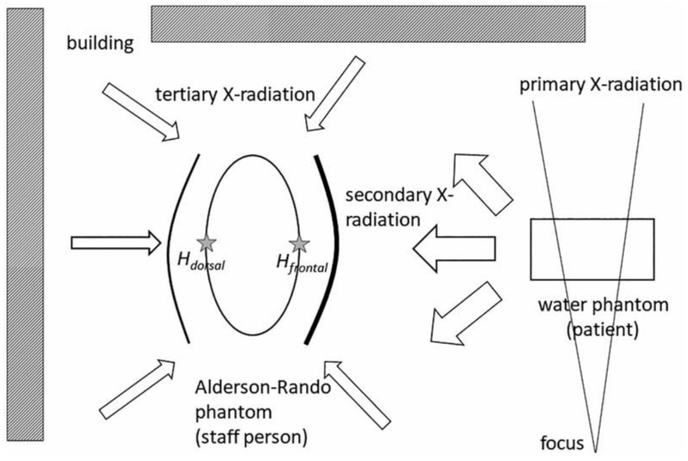

Figure 1. The radiation components of a treatment room: primary, secondary, and tertiary radiation [5].

How it works

- The MC methods we will be focusing on are the Geant4 and the PENELOPE MC codes.
- The MC method works by randomly sampling the space and calculating the dose at each point. At each point, 2 dimensional ray cast is done starting from the source and ending at the point of interest.
- Interactions, overlaying many physical processes that occur to the particle in flight before being absorbed, such as rayleigh scattering, photoelectric effect, Compton scattering, and pair production, as well as attenuation due to the material the particle is passing through, are calculated at each [variable] time step [1].
- We simulate the movement of the particle until a process occurs - either interaction, decay, or continuous energy loss.
- We run the process to determine the outcome that lead to the smallest step size (the first thing that happens) and then move the particle that distance [3].
- Dependent on what the process was, we then choose what to do:
  - If the process was an interaction or a decay, the particle is killed and secondary particles are created if necessary.
  - If the process was continuous energy loss, the particle's energy is updated and the step size is recalculated.

  This post-step process is very similar to that of a recursive ray tracing algorithm.
- Once the energy of a particle falls below a given absorption threshold $E_{abs,P}$, the tracking of the particle is stopped [1]. Once the particle is killed, we calculate fluence at the point of interest and add it to the current fluence.
- This allows us to create an isodose map of the room. If we're looking for the dose that a person would receive, we can add a volume to the simulation and calculate the dose to that volume through a numeric surface integral.

Numerical approximation of particle interactions

These physical processes are modelled using probability distributions. In order to determine these probability distributions, we consider two different and independent molecular differential cross-sections (denoted as A and B) to develop the following scattering model:

$$\frac{\mathrm{d}^2\sigma_{\mathrm{A}}(E;\theta,W)}{\mathrm{d}\Omega\mathrm{d}W} \quad \text{and} \quad \frac{\mathrm{d}^2\sigma_{\mathrm{B}}(E;\theta,W)}{\mathrm{d}\Omega\mathrm{d}W} \tag{1}$$

where $d\Omega$ is a solid angle in the direction (θ,ϕ) and W is the energy loss of the particle [1]. This then gives us a PDF for the scattering angle θ and energy loss W for a given scattering event:

$$p_{\mathrm{A,B}}(E;\theta,W) = \frac{2\pi\sin\theta}{\sigma_{\mathrm{A,B}}(E)}\frac{\mathrm{d}^2\sigma_{\mathrm{A,B}}(E;\theta,W)}{\mathrm{d}\Omega\mathrm{d}W}. \tag{2}$$

In order to model the final state of the particle, we can either choose a data driven model, a semi-empirical model, or a model based on the physics of the process to determine the PDF functions [3].

Once we have completed the MC simulation (MCS), a transformation from the fluence to the dose is required. We consider particles only above a certain energy threshold Δp, that is not necessarily the same as the absorption threshold $E_{abs,P}$. Then, given the total fluence distribution with respect to the energy of particles at point $\mathbf{r}$ denoted as $\Phi_P(\mathbf{r},E)$, the absorbed dose at point $\mathbf{r}$ is given by:

$$D(\mathbf{r}) = \frac{1}{\rho(\mathbf{r})}\sum_P \int A_{\Delta,P}(E)\Phi_P(\mathbf{r},E)\mathrm{d}E \tag{3}$$

where $A_{\Delta,P}(E)$ is the average energy that is transferred to the material per unit path length, $\rho(\mathbf{r})$ is the density of the material at point $\mathbf{r}$, and P is the particle type [1]. In practice, this simplifies to a simple numeric calculation for the dose given a direct proportionality between the number of particles and the dose [14].

Geometric Modelling of the Treatment Room

There are several methods that can be chosen to model the treatment room, each with varying levels of computational complexity. The simplest method is to model the room as a series of voxels, where each voxel is a cube of a given size. Figure 2 shows a voxel model of a treatment room.

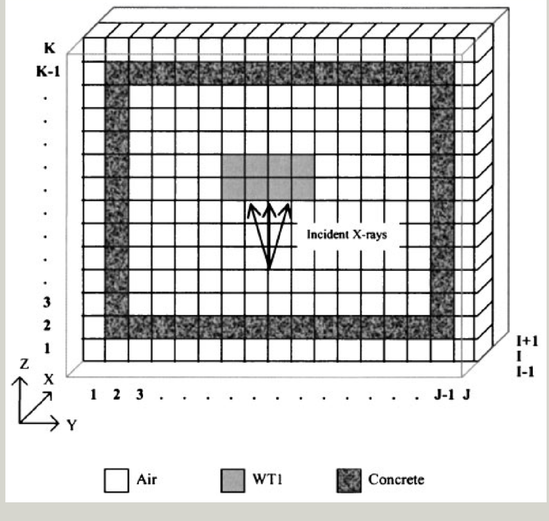

Figure 2. A voxel model of a treatment room [10].

Accuracy of this particular method somewhat increases as we increase the size of the voxels. The voxel method is good when it accurately reflects the room geometry.

However, when we are computing reflections off an object, the normal of the surface is not in the same direction as the true surface normal unless the only volumes we are considering are flat and parallel to the x, y, and z axes. It is likely that this does not accurately reflect the true geometry of the room, treatment device, and personnel. As we can see in Figure 2, the patient is modelled with voxels - this is a very rough approximation of the patient's true geometry. Earlier studies noted the geometric and compositional complexity of treatment devices and the inherent inaccuracy of trying to model such devices [2]. As a result, these methods also ignored scatter from the x-ray collimator due to geometric limitations, which lead to underestimation of the scatter in a particular study [10].

We can improve the accuracy of the model by using more complex geometries, such as polygonal meshes or B-spline surfaces [3, 7]. Geant4, for example, allows for the use of CAD systems to model the treatment room geometry. PENELOPE also allows for more complex geometries to be used in the MCS. Voxelization can therefore, if needed, be used as a computational optimization for flat surfaces as opposed to the only method of modelling the overall room geometry.

Practicality of Numerical Methods

Increases in workloads in x-ray facilities increase the need for quantification of tertiary scatter [5] The use of MCSs to model the treatment room is a computationally intensive process, and not every physical process is modelled in previous MCSs (such as beam filtration). However, when the treatment room is modelled using accurate geometry, measurements of air kerma show agreement with the MCS [9].

This leads to the bottleneck of computation time in such simulations as a result of increased geometric complexity. MC simuations have been shown to be accurate when the geometry is accurate in the simulation, as discussed above, but even modern simulations have long runtimes. An assessment of scattered radiation from hand-held dental x-ray equipment using the MC method, for example, took 72 hours to run on a relatively modern CPU [4].

These are similar bottlenecks to those seen in other geometric modelling methods, such as ray tracing. The CPU is not directly designed for the sheer scale of parallelism that is possible in MCSs. Hardware that is specially designed for the task of parallelization for SIMD (single instruction, multiple data) operations, such as GPUs, can be used to speed up the simulation. A recent study researching the use of GPUs for MCSs have shown that the use of GPUs can speed up the simulation by a factor of 2363 [13]. It was, however, hindered by thread divergence, due to the stochastic nature of the simulation. These are similar hindrances to those seen in ray tracing, which tends to have high thread divergence due to the nature of the algorithm [8].

Recent developments in GPU hardware have lead to the capabilities of real-time ray tracing on dedicated GPUs [11]. Given the incredible amount of similarity between the two algorithms, it is likely that the same techniques used to speed up ray tracing can be used to speed up MCSs. Further research is required to determine the practicality of using GPUs with dedicated ray tracing hardware to speed up MCSs, as well as a re-assessed cost-benefit analysis of the use of MCSs in the treatment room given developments to significantly decrease the computation time.

References

[1] Nuclear Energy Agency. *PENELOPE 2018: A code system for Monte Carlo simulation of electron and photon transport*. Nuclear Energy Agency, 2019. doi:https://doi.org/https://doi.org/10.1787/32da5043-en. URL https://www.oecd-ilibrary.org/content/publication/32da5043-en.

[2] S. Agosteo, A. Foglio Para, B. Maggioni, V. Sangiust, S. Terrani, and G. Borasi. Radiation transport in a radiotherapy room. *Health physics*, 68(1):27–34, 1995. doi:10.1097/00004032-199501000-00003.

[3] S. Agostinelli, J. Allison, K. Amako, et al. Geant4—a simulation toolkit. *Nuclear Instruments and Methods in Physics Research Section A: Accelerators, Spectrometers, Detectors and Associated Equipment*, 506(3):250–303, 2003. ISSN 0168-9002. doi:https://doi.org/10.1016/S0168-9002(03)01368-8. URL https://www.sciencedirect.com/science/article/pii/S0168900203013688.

[4] W. O. Batista, M. R. Soares, J. M. G. Rios, A. C. D. S. Souza, I. M. Pinheiro, J. L. J. V. Ramirez, and L. V. E. Caldas. Assessment of scattered radiation from hand-held dental x-ray equipment using the monte carlo method. *Journal of radiological protection : official journal of the Society for Radiological Protection*, 41(4):10.1088/1361–6498/abf3cd, 2021. doi:10.1088/1361-6498/abf3cd.

[5] H. Eder, M. Seidenbusch, and L. S. Oechler. Tertiary x-radiation-a problem for staff protection? *Radiation protection dosimetry*, 189(3):304–311, 2020. doi:10.1093/rpd/ncaa043.

[6] B. A. Faddegon, I. Kawrakow, Y. Kubyshin, J. Perl, J. Sempau, and L. Urban. The accuracy of egsnrc, geant4 and penelope monte carlo systems for the simulation of electron scatter in external beam radiotherapy. *Physics in medicine and biology*, 54(20):6151–6163, 2009. doi:10.1088/0031-9155/54/20/008.

[7] William J. Gordon and Richard F. Riesenfeld. B-spline curves and surfaces. In ROBERT E. BARNHILL and RICHARD F. RIESENFELD, editors, *Computer Aided Geometric Design*, pages 95–126. Academic Press, 1974. ISBN 978-0-12-079050-0. doihttps://doi.org/10.1016/B978-0-12-079050-0.50011-4. URL https://www.sciencedirect.com/science/article/pii/B9780120790500500114.

[8] Roman Malits, Evgeny Bolotin, Avinoam Kolodny, and Avi Mendelson. Exploring the limits of gpgpu scheduling in control flow bound applications. *TACO*, 8:29, 01 2012. doi:10.1145/2086696.2086708.

[9] C J Martin, D G Sutton, J Magee, S McVey, J R Williams, and D Peet. Derivation of factors for estimating the scatter of diagnostic x-rays from walls and ceiling slabs. *Journal of Radiological Protection*, 32(4):373, sep 2012. doi:10.1088/0952-4746/32/4/373. URL https://dx.doi.org/10.1088/0952-4746/32/4/373.

[10] G. McVey and H. Weatherburn. A study of scatter in diagnostic x-ray rooms. *The British journal of radiology*, 77(913):28–38, 2004. doi:10.1259/bjr/93969091.

[11] NVIDIA. Geforce rtx | ultimate ray tracing & ai | nvidia, 2022. URL https://www.nvidia.com/en-us/geforce/rtx/.

[12] H. Paganetti, H. Jiang, K. Parodi, R. Slopsema, and M. Engelsman. Clinical implementation of full monte carlo dose calculation in proton beam therapy. *Physics in medicine and biology*, 53(17):4825–4853, 2008. doi:10.1088/0031-9155/53/17/023.

[13] M. Shi, M. Myronakis, M. Jacobson, D. Ferguson, C. Williams, M. Lehmann, P. Baturin, P. Huber, R. Fueglistaller, I. V. Lozano, T. Harris, D. Morf, and R. I. Berbeco. Gpu-accelerated monte carlo simulation of mv-cbct. *Physics in medicine and biology*, 65(23):235042, 2020. doi:10.1088/1361-6560/abaeba.

[14] Y. Wang, L. E. Antonuk, Y. El-Mohri, Q. Zhao, A. Sawant, and H. Du. Monte carlo investigations of megavoltage cone-beam ct using thick, segmented scintillating detectors for soft tissue visualization. *Medical physics*, 35(1):145–158, 2008. doi:10.1118/1.2818957.